Mon. Not. R. Astron. Soc. **000**, **??**–**??** (2016) Printed 2 January 2017 (MN LATEX style file v2.2)

# The X-ray Decay of the Ultraluminous Supernova SN 1978K in NGC 1313

Hai-Hui Zhao[1], Shan-Shan Weng[1⋆], C.-Y. Ng[2]
[1] *Department of Physics and Institute of Theoretical Physics, Nanjing Normal University, Nanjing 210023, China*
[2] *Department of Physics, The University of Hong Kong, Pokfulam Road, Hong Kong*

arXiv:1612.09473v1 [astro-ph.HE] 30 Dec 2016

**ABSTRACT**

The Type IIn supernova (SN) 1978K in the nearby galaxy NGC 1313 has remained bright in multi-wavelengths for more than $\sim 25$ years. The archival data of SN 1978K collected with *ROSAT*, *ASCA*, *XMM-Newton*, and *Chandra* from 1990 to 2006 show no significant variation of the soft X-ray emission but a hint of flux decrease in hard X-rays. In this work, we perform a detailed analysis using more than 15 years of *XMM-Newton* observations. Both the 0.5-2 keV and 2-10 keV light curves decline as of $t^{-1}$ from 2000 to 2015. The transition of light curve profiles can be explained in the way that the reverse shock was radiative at early phase and then became adiabatic at late times. Such a scenario is also supported by the spectral analysis results. We also found a decrease in the absorption column density, which indicates the presence of a cool shell during the radiative phase.

**Key words:** circumstellar matter — supernovae: individual (SN 1978K) — X-rays: stars

## 1 INTRODUCTION

Progenitors of supernovae (SNe), massive stars **lose** mass via stellar winds, forming circumstellar medium (CSM). After the explosion, the SN shock waves expand into the surrounding CSM (see reviews by Smith 2014). The subsequent interaction creates a fast forward and a reverse shocks (e.g. Chevalier & Fransson 1994; Chatzopoulos et al. 2012). Such interaction can be investigated with radio, infrared, ultraviolet, and X-ray observational data (e.g. Chugai et al. 2007; Tanaka et al. 2012; Milisavljevic et al. 2013; Ng et al. 2013; Gezari et al. 2015; Ryder et al. 2016). If the SNe propagate in the steady stellar winds, we would expect that the X-ray luminosity resulting from shocks declines in a power-law way. Recently, Dwarkadas & Gruszko (2012) collected the X-ray data of 42 SNe and found diverse light curve profiles. There are increasing evidences that the density structure of the ambient medium may not follow $r^{-2}$ as expected according to the steady wind theory (Chevalier & Fransson 2003; Chandra et al. 2009). It can even be inhomogeneous or clumpy.

SN 1978K was first discovered as a strong H$\alpha$ source in 1990 during a spectrophotometric survey of H II region in nearby galaxies, and it was originally classified as a nova (Dopita & Ryder 1990). Investigating the multi-wavelength archival data, Ryder et al. (1993) suggested that it was actually a Type II SN which exploded around 1978 May 22 (Montes et al. 1997). Based on the X-ray and radio data, Schlegel et al. (1999) suggested that the behavior of SN 1978K is typical of the "IIn" subclass of Type II SN, which was first designated by Schlegel (1990). The powerful non-thermal radio emission was first revealed with the Molonglo Observatory Synthesis Telescope data taken in 1982 (Ryder et al. 1993). It reached a peak luminosity around the late 1980s, and then declined monotonically up to now (Smith et al. 2007). On the 1980 January 2, the *Einstein* X-ray satellite observed the region of SN 1978K, and obtained an upper limit of unabsorbed flux in 0.2–2.4 keV of $1.1 \times 10^{-13}$ erg cm$^{-2}$ s$^{-1}$. X-ray emission of SN 1978K was uncovered with *ROSAT* Position Sensitive Proportional Counter in 1990 (Ryder et al. 1993; Lenz & Schlegel 2007). The derived unabsorbed flux was of $\sim 10^{-12}$ erg cm$^{-2}$ s$^{-1}$ in the 0.2–2.4 keV range, that is $\sim 3 \times 10^{39}$ erg s$^{-1}$ at a distance of 4.61 Mpc (Gao et al. 2015), identifying SN 1978K as an ultraluminous X-ray source (ULX). Follow-up X-ray observations made with *ASCA*, *XMM-Newton*, and *Chandra* indicated that the X-ray luminosity of SN 1978K remains bright even at $\sim 37$ years after the explosion (e.g. Lenz & Schlegel 2007; Smith et al. 2007).

Since SN 1978K is luminous in multi-wavelength, the long-term broadband monitoring data provide a good opportunity for the study of the interaction between the outgoing shock and the CSM. The X-ray data of SN 1978K prior to 2006 have been analyzed; however, whether its flux remain constant since the first detection by *ROSAT* or started to decline was still under debate (e.g. Lenz & Schlegel 2007; Smith et al. 2007). It is worth noting that there are another two ULXs (X-1 and X-2) in NGC 1313. Thus, this region has been frequently visited by X-ray missions in order to explore the spectral evolution of these sources (e.g. Feng & Kaaret 2006; Bachetti 2013; Weng et al. 2014). In the past decade, some additional long observations were carried out with *XMM-Newton*

⋆ E-mail: wengss@njnu.edu.cn

(Table 1), which is a focusing X-ray telescope having a large effective area in the soft X-ray band. In this paper, we study the *XMM-Newton* observations covering from 2000 to 2015 (spanning 5277 days) aiming to explore the evolution in X-ray emission of SN 1978K at very late times. The *XMM-Newton* data reduction is described in the next section, and the results are presented in Sections 3. Discussion and conclusion follow in Section 4.

## 2 DATA REDUCTION

The detailed study presented here was on data from the main camera onboard *XMM-Newton*, the European Photon Imaging Camera (EPIC), which consists of two MOS and one PN CCD arrays (Strüder et al. 2001; Turner et al. 2001). We analyze all of the available *XMM-Newton* observations of SN 1978K made from 2000 October to 2015 March; however, we discard those data which were affected by the strong background flares or when the source falls in the CCD gaps. The observational details of the data used in this paper are listed in Table 1. The *XMM-Newton* observations of SN 1978K are quite clean except two short data observed in 2003 December (ObsIDs = 0150280401, 0150280501), and only less than 12% of data on average are excluded. The data are reduced with the Science Analysis System software (SAS) version 14.0.0. We create the light curve above 10 keV, and exclude background flares with a count rate cut-off criterion. The data from good time intervals are filtered by setting FLAG = 0 and PATTERN $\leqslant$ 4 for the PN data, and PATTERN $\leqslant$ 12 for the MOS data to ensure the best quality spectrum (Snowden et al. 2016). The source photons are extracted from a circle aperture with a radius of $30''$, while the background is taken from the same CCD chips as the source and at a similar distance from the readout node. Since the source is relatively faint ($flux < 10^{-12}$ erg cm$^{-2}$ s$^{-1}$), the pile-up effect can be neglected. We produce the response files with the SAS tasks `rmfgen` and `arfgen` to facilitate subsequent spectral analysis. The task `specgroup` is carried out to rebin all spectra to have at least 20 counts per bin and not to oversample the instrument energy resolution by more than a factor of three.

We fit the spectra in the 0.5–10 keV range using XSPEC with a 2% systematic error added (Smith et al. 2016). When available, the PN and MOS spectra for each observation are fitted together. To account for the cross-normalization issues, we include a multiplicative constant in the model and fix it to unity for the PN data, but allow it to vary for the MOS data. Due to the short exposure time, it is difficult to constrain the parameters for the individual observation carried out before 2006. Since there is no significant spectral evolution within less than one year, we merge some successive observations, which are referred to as Groups 1-8 (Tables 1 and 2), to better constrain the model parameters.

The X-ray emission from SN 1978K can be described by an absorbed two-temperature optically thin thermal plasma model, in which the soft and hard components are attributed to the reverse and forward shocks, respectively. Smith et al. (2007) suggested the X-ray spectra of SN 1978K can be fitted with a double `vmekal` model (see also Schlegel et al. 2004) with very large helium abundance. Here, we first apply a two-temperature non equilibrium ionization model (`vnei` in XSPEC), and confirmed that helium abundance in both components needs to be large. The ionization timescale for the soft component is larger $3 \times 10^{13}$ s cm$^{-3}$, indicating that the reverse shock collides with very dense clouds and has already reached ionization equilibrium. Meanwhile, the ionization timescale for the hard component is $\sim (5-10)\times10^{10}$ s cm$^{-3}$, indicating a non-equilibrium condition. Therefore, we adopt the `tbabs*(vmekal+vnei)` model in the following spectra analysis, since `vnei` reduces to `vmekal` in ionization equilibrium and the latter is much faster to compute.

The best-fit spectral parameters with uncertainties at 90% confidence level are listed in Table 2. Both the absorbed and unabsorbed fluxes are calculated with convolution model `cflux`. The evolution of the X-ray luminosity and the equivalent hydrogen column density are not sensitive to the spectral models, while the parameters of two shocks, including plasma temperatures and large He abundances, generally agree with those by Smith et al. (2007), who also gave an all-round analysis of the *XMM-Newton* data prior to 2006. However, there is no evidence for the large He abundances detected in the *Chandra* data (Schlegel et al. in preparation). The divergence might be due to the calibration differences between *Chandra* and *XMM-Newton* (e.g. Nevalainen et al. 2010; Schellenberger et al. 2015). Note that our absorption column density ($N_{\rm H} \sim (2.1-2.5) \times 10^{21}$ cm$^{-2}$) is slightly higher than the values reported in Smith et al. (2007) and Lenz & Schlegel (2007), due to the choice of the updated solar abundances by Wilm et al. (2000). This value is also much larger than the absorption in the direction of NGC1313, $\sim 3.7 \times 10^{20}$ cm$^{-2}$ (Schlegel et al. 1998).

## 3 RESULTS

Since the first *XMM-Newton* observation carried out on 2000 October 17, the X-ray flux of SN 1978K had dropped by 40% in the last 15 years. Assuming a distance of 4.61 Mpc (Gao et al. 2015), the unabsorbed luminosity in 0.5–10 keV band are 2.96 $\times10^{39}$ erg s$^{-1}$ and 1.76 $\times10^{39}$ erg s$^{-1}$ on 2000 October 17 and 2015 March 30. The detailed flux evolution is plotted in Figure 1. It is quite obvious that the unabsorbed X-ray fluxes of SN 1978K display a power-law decay. Using the IDL routine `linfit`, we fit the light curves with the following function

$$\log(flux) = A(0) \times \log(t - t_0) + A(1), \qquad (1)$$

where $t$ is the observational date in days, $t_0$ is taken to be MJD 43,650 (1978 May 22; Montes et al. 1997) when the SN was at peak luminosity, $A(0)$ and $A(1)$ are the fitting parameters. The derived values of $A(0)$ are $-1.02 \pm 0.15$ for 0.5–2 keV, and $-1.24 \pm 0.10$ for 2–10 keV. In Figure 1, we also plot the X-ray fluxes measured by *Einstein*, *ROSAT*, and *ASCA* (Schlegel et al. 2004, and references therein). These archival data indicate that the X-ray flux in 0.5–2 keV band had a shallower decay or remained constant at earlier stage. On the other hand, the 2–10 keV flux estimated from the ASCA data could be consistent with the extrapolated value of our power-law fitting (bottom panel of Figure 1).

As seen in Table 2, the absorption column density ($N_{\rm H}$) decreases with time. It is worth noting that the parameters in Groups 1-4 (and 5-8) vary by less than 20%. Therefore, in order to increase the signal-to-noise ratio, we divide all spectra into two parts, those collected before 2006 October 16 and those between 2012 and 2015. The same spectral model is then applied to these two sets of spectra (Table 3), respectively. We found that the value of $N_{\rm H}$ decreases by more than $5\sigma$ (from 2.53 to 2.12 $\times10^{21}$ cm$^{-2}$) over the last $\sim$ 10 years. However, we can not estimate the evolution of the parameters of the hot plasma components because of their large uncertainties.

| Group | ObsID | Obs Date | Instruments | Net Exposure (ksec) |
|---|---|---|---|---|
| Group1 | 0106860101 | 2000-10-17 | PN/MOS1/MOS2 | 24.1/28.7/28.7 |
| Group2 | 0150280301 | 2003-12-21 | PN/MOS1/MOS2 | 7.7/10.5/10.5 |
| .. | 0150280401 | 2003-12-23 | PN/MOS1/MOS2 | 3.3/8.1/8.5 |
| .. | 0150280501 | 2003-12-25 | PN/MOS1/MOS2 | 6.4/9.3/9.4 |
| .. | 0150280601 | 2004-01-08 | PN/MOS1/MOS2 | 8.4/12.8/13.0 |
| .. | 0150281101 | 2004-01-16 | MOS1/MOS2 | 8.5/8.5 |
| .. | 0205230201 | 2004-05-01 | MOS1/MOS2 | 8.7/9.3 |
| Group3 | 0205230301 | 2004-06-05 | PN/MOS1/MOS2 | 8.9/11.6/11.5 |
| .. | 0205230401 | 2004-08-23 | PN/MOS1/MOS2 | 9.0/14.9/15.2 |
| .. | 0205230501 | 2004-11-23 | MOS1/MOS2 | 15.5/15.5 |
| .. | 0205230601 | 2005-02-07 | PN/MOS1/MOS2 | 9.8/12.6/12.9 |
| Group4 | 0301860101 | 2006-03-06 | PN/MOS1/MOS2 | 17.5/21.3/21.3 |
| .. | 0405090101 | 2006-10-15 | PN/MOS1/MOS2 | 86.0/119.0/119.6 |
| Group5 | 0693850501 | 2012-12-16 | PN/MOS1/MOS2 | 97.9/117.7/120.2 |
| .. | 0693851201 | 2012-12-22 | PN/MOS1/MOS2 | 101.4/121.1/123.7 |
| Group6 | 0722650101 | 2013-06-08 | PN/MOS1/MOS2 | 20.0/30.1/30.1 |
| Group7 | 0742590301 | 2014-07-05 | PN/MOS1/MOS2 | 53.6/61.0/61.1 |
| Group8 | 0742490101 | 2015-03-30 | PN/MOS1/MOS2 | 84.8/98.0/100.1 |

**Table 1.** XMM-Newton Observations of SN 1978K. Net exposure: clean exposure after background flares excluded.

| ObsID | $N_{\rm H}$ ($10^{21}$ cm$^{-2}$) | $kT_{\rm soft}$ (keV) | $\rm He_{soft}$ | $kT_{\rm hard}$ (keV) | $\rm He_{hard}$ | $\log(\tau_{\rm hard})$ (s cm$^{-3}$) | $flux^{\sharp}_{0.5-2\rm keV}$ ($10^{-13}$ erg cm$^{-2}$ s$^{-1}$) | $flux^{\sharp}_{2-10\rm keV}$ ($10^{-13}$ erg cm$^{-2}$ s$^{-1}$) | $\chi^2$/dof |
|---|---|---|---|---|---|---|---|---|---|
| Group1 | $2.70^{+0.39}_{-0.38}$ | $0.63^{+0.03}_{-0.04}$ | $29^{+12}_{-9}$ | $4.0^{+1.2}_{-0.8}$ | $49^{+54}_{-22}$ | $10.8^{+0.1}_{-0.2}$ | $4.27^{+0.09}_{-0.09}/7.6^{+0.7}_{-0.7}$ | $3.11^{+0.22}_{-0.20}/3.19^{+0.22}_{-0.20}$ | 129.5/165 |
| Group2 | $2.54^{+0.38}_{-0.38}$ | $0.60^{+0.03}_{-0.03}$ | $29^{+10}_{-9}$ | $4.7^{+1.4}_{-1.0}$ | $22^{+37}_{-16}$ | $11.1^{+0.3}_{-0.2}$ | $3.93^{+0.10}_{-0.10}/6.8^{+0.7}_{-0.6}$ | $3.11^{+0.23}_{-0.22}/3.17^{+0.23}_{-0.22}$ | 467.4/431 |
| Group3 | $2.65^{+0.43}_{-0.35}$ | $0.57^{+0.03}_{-0.05}$ | $33^{+12}_{-10}$ | $3.7^{+0.8}_{-0.6}$ | $64^{+102}_{-34}$ | $10.9^{+0.2}_{-0.3}$ | $3.90^{+0.08}_{-0.08}/7.0^{+0.8}_{-0.6}$ | $2.73^{+0.17}_{-0.16}/2.80^{+0.17}_{-0.16}$ | 413.9/401 |
| Group4 | $2.52^{+0.23}_{-0.22}$ | $0.59^{+0.02}_{-0.03}$ | $30^{+7}_{-6}$ | $3.7^{+0.4}_{-0.3}$ | $106^{+67}_{-40}$ | $10.7^{+0.2}_{-0.2}$ | $3.87^{+0.04}_{-0.04}/6.7^{+0.4}_{-0.4}$ | $2.76^{+0.09}_{-0.09}/2.82^{+0.09}_{-0.09}$ | 450.6/413 |
| Group5 | $2.06^{+0.15}_{-0.16}$ | $0.63^{+0.01}_{-0.01}$ | $24^{+4}_{-4}$ | $3.4^{+0.3}_{-0.3}$ | $42^{+41}_{-31}$ | $11.1^{+0.5}_{-0.2}$ | $3.26^{+0.03}_{-0.03}/5.1^{+0.2}_{-0.2}$ | $1.96^{+0.05}_{-0.05}/2.00^{+0.05}_{-0.05}$ | 507.6/481 |
| Group6 | $2.32^{+0.39}_{-0.47}$ | $0.63^{+0.03}_{-0.03}$ | $30^{+12}_{-13}$ | $3.6^{+1.3}_{-0.9}$ | $9^{+246}_{-6}$ | $11.5^{+2.2}_{-0.3}$ | $3.15^{+0.08}_{-0.08}/5.3^{+0.5}_{-0.6}$ | $1.95^{+0.16}_{-0.17}/1.99^{+0.16}_{-0.17}$ | 169.1/143 |
| Group7 | $2.35^{+0.28}_{-0.28}$ | $0.65^{+0.02}_{-0.02}$ | $26^{+7}_{-6}$ | $4.1^{+1.3}_{-0.7}$ | $6^{+19}_{-4}$ | $11.6^{+2.1}_{-0.4}$ | $3.06^{+0.05}_{-0.05}/5.1^{+0.4}_{-0.3}$ | $1.93^{+0.12}_{-0.11}/1.97^{+0.12}_{-0.11}$ | 208.1/177 |
| Group8 | $2.08^{+0.23}_{-0.23}$ | $0.61^{+0.02}_{-0.02}$ | $20^{+5}_{-5}$ | $3.4^{+0.4}_{-0.3}$ | $35^{+28}_{-15}$ | $11.1^{+0.2}_{-0.2}$ | $2.96^{+0.04}_{-0.04}/4.7^{+0.3}_{-0.3}$ | $1.92^{+0.06}_{-0.06}/1.96^{+0.07}_{-0.06}$ | 214.3/236 |

**Table 2.** Best-fit spectral parameters of SN 1978K with the model of `tbabs*(vmekal+vnei)`. ♯: Both absorbed (former) and unabsorbed (latter) fluxes are calculated in the 0.5–2 keV and 2–10 keV, respectively. All errors are in the 90% confidence level.

## 4 DISCUSSION AND CONCLUSION

Multiband observations of type II SNe bear the imprint of interaction between the SNe and CSM ejected by their progenitors. For non-radiative case, we would expect that the X-ray emission decreases inversely with time as $t^{-1}$ if SNe expand into a steady wind medium (see e.g. Immler & Lewin 2003). Dwarkadas & Gruszko (2012) investigated the light curves of 42 SNe, but found none of them declines as $L_{\rm X} \propto t^{-1}$. Before our work, Lenz & Schlegel (2007) claimed that the soft X-ray flux of SN 1978K remained at a constant level, whereas the hard X-ray emission dropped slightly. In the meantime, the radio light curves faded steadily since 1991 (Smith et al. 2007) [1]. Here, we analyze all archival *XMM-Newton* data for both light curve and spectral evolution. It is remarkable that both the soft and hard X-ray light curves turn into a $t^{-1}$ decline around the year 2000 ($\sim 6000-8000$ days after explosion). This result implies that the shock wave is now propagating through the medium with a density gradient $r^{-2}$ (Chevalier & Fransson 2003; Chandra et al. 2009; Dwarkadas & Gruszko 2012), and the free-free radiation dominates the X-ray emission. Alternatively, transition of the reverse shock from radiative to adiabatic phases could account for the change of the light curve decay rate. As we discuss below, such a scenario is supported by both the temporal and spectral evolution, and it was proposed to explain the behavior of SN 1993J (Chandra et al. 2009).

SN 1993J is another bright SN and is well studied in broadband wavelength (e.g., Jerkstrand et al. 2015; Bjornsson 2015, and references therein). During the first $\sim$ 5 years, the soft and hard X-ray fluxes had shallow decays at different rates, and then both underwent a $t^{-1}$ decline at later times (Chandra et al. 2009), analogous to what SN 1978K exhibits (Figure 1). With the self-similar assumption of steady progenitor wind, the free-free emission from the adiabatic shock is suggested to follow time evolution of $t^{-1}$ (e.g. Chevalier & Fransson 2003). The forward shock, corresponding to the harder component, is in the adiabatic phase since the very beginning. On the other hand, the reverse shock (the softer component) could be radiative at the early stage having a flatter profile of soft X-ray light curve, and then it becomes adiabatic after a cooling time of the gas behind the reverse shock (Chandra et al. 2009).

The caution is that SN 1993J is categorized as a Type IIb

[1] https://www.ast.cam.ac.uk/ioa/wikis/SEES/images/f/f1/Ryder.pdf

| Date | $N_{\rm H}$ ($10^{21}$ cm$^{-2}$) | $kT_{\rm soft}$ (keV) | He$_{\rm soft}$ | norm$_{\rm soft}$ ($\times10^{-4}$) | $kT_{\rm hard}$ (keV) | He$_{\rm hard}$ | $\log(\tau_{\rm hard})$ (s cm$^{-3}$) | norm$_{\rm hard}$ ($\times10^{-4}$) | $\chi^2$/dof |
|---|---|---|---|---|---|---|---|---|---|
| 2000-2006 | $2.53^{+0.15}_{-0.15}$ | $0.60^{+0.01}_{-0.01}$ | $29^{+4}_{-4}$ | $1.21^{+0.06}_{-0.06}$ | $3.9^{+0.3}_{-0.3}$ | $68^{+33}_{-21}$ | $10.9^{+0.1}_{-0.1}$ | $0.19^{+0.08}_{-0.06}$ | 1643.5/1437 |
| 2012-2015 | $2.12^{+0.11}_{-0.11}$ | $0.63^{+0.01}_{-0.01}$ | $23^{+3}_{-3}$ | $0.99^{+0.04}_{-0.04}$ | $3.5^{+0.2}_{-0.2}$ | $41^{+22}_{-21}$ | $11.1^{+0.3}_{-0.1}$ | $0.23^{+0.21}_{-0.07}$ | 1257.7/1064 |

**Table 3.** Same as Table 2 but with spectra re-grouped.

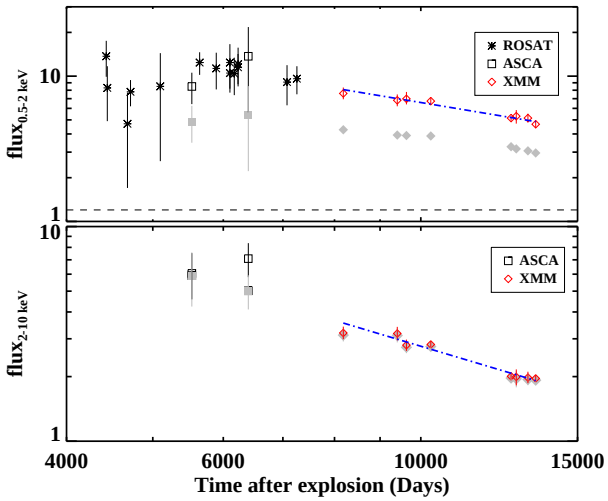


**Figure 1.** 0.5–2 keV (upper panel) and 2–10 keV (bottom panel) X-ray fluxes in units of $10^{-13}$ erg cm$^{-2}$ s$^{-1}$ versus SN age. The black data points mark the unabsorbed fluxes from other X-ray missions (adopted from Schlegel et al. 2004, and references therein), and grey solid symbols correspond to the absorbed fluxes. The horizontal dashed line in the upper panel represents the upper limit derived from the *Einstein* IPC observation on 1980 January 2 (age $\sim$ 590 days). The red points are from this paper (Table 2), which can be fitted by a power-law decay (blue dot-dashed lines).

SN (Woosley et al. 1994), while SN 1978K is a Type IIn. SN 1978K is still barely resolved in the new VLBI image at 8.4 GHz on 2015 Mrach 29; therefore, Ryder et al. (2016) suggested that its average expansion velocity in last 37 years is less than 1500 km s$^{-1}$. Compared to the case in SN 1993J, the much slower shock velocity of $\sim$ 500–600 km s$^{-1}$ in SN 1978K shown by the optical emission lines indicates that the SN blast wave has been decelerated by the very dense CSM (Chugai et al. 1995; Kuncarayakti et al. 2016). Since the cooling time of the gas behind the reverse shock is anti-correlated with the shock velocity ($t_{\rm c} \propto v_{\rm s}^{-5.2}$; Chevalier & Fransson 1994; Chandra et al. 2009), the lower shock speed in SN 1978K results in the longer transition time ($\sim$ 6000 – 8000 days; Figure 1) for radiative cooling. In addition, the large He abundances observed in SN 1978K (Table 3) would extend the cooling time further (see Table 3 in Chandra et al. 2009).

In the radiative regime, the existence of a cooled shell between the reverse and forward shocks gives rise to additional X-ray absorption, and the column density of the cool gas reduces with time as the SN expands (Chevalier & Fransson 1994; Fransson et al. 2006; Chandra et al. 2009). With the high quality spectra collected by *XMM-Newton*, our result provides, for the first time, a strong evidence for the decrease of absorption over the last decade (Table 3), that well agrees with the model discussed above. We further speculate that the non-detection of SN 1978K on 1980 January 2 could be due to the large absorption by the cool shell.

## ACKNOWLEDGEMENTS

We thank the referee, Prof. Eric M. Schlegel, for the helpful comments. We thank Drs. Ming-Yu Ge and Qi-Rong Yuan for many valuable suggestions. This work is supported by the National Natural Science Foundation of China under grants 11303022, 11133002, 11573023, 11173016, 11673013 and 11433005, and by the Special Research Fund for the Doctoral Program of Higher Education (grant No. 20133207110006).

## REFERENCES

Bachetti, M., Rana, V., Walton, D. J., et al. 2013, ApJ, 778, 163
Bjornsson C. I., 2015, ApJ, 813, 43
Chandra, P., Dwarkadas, V. V., Ray, A., Immler, S., & Pooley, D. 2009 , ApJ, 699, 388
Chatzopoulos, E., Wheeler, J. C., & Vinko, J. 2012, ApJ , 746, 121
Chevalier R. A., & Fransson C., 1994, ApJ, 420, 268
Chevalier,R., & Fransson, C. 2003, in Lecture Notes in Physics 598, Supernovae and Gamma-Ray Bursters, ed. K. Weiler (Berlin: Springer-Verlag), 171
Chugai, N. N., Chevalier, R. A., & Utrobin, V. P. 2007, ApJ, 662, 1136
Chugai, N. N., Danziger, I. J., & della Valle, M. 1995, MNRAS, 276, 530
Dopita, M. A., & Ryder, S. D. 1990, IAU Circ., 4950, 3
Dwarkadas, V. V., & Gruszko, J. 2012, MNRAS, 419, 1515
Feng, H., & Kaaret, P. 2006, ApJ, 650, L75
Fransson, C., Lundqvist, P., & Chevalier, R. A. 1996, ApJ, 461, 993
Gao, Q., Wang, W., Liu, J.-F., & Yoachim, P. 2015, ApJ, 799, 19
Gezari, S., Jones, D. O., Sanders, N. E., et al. 2015, ApJ, 804, 28
Immler S., & Lewin W. H. G., 2003, in Weiler K., ed., Lecture Notes in Physics, Vol. 598, Supernovae and Gamma-Ray Bursters. Springer- Verlag, Berlin, p. 91
Jerkstrand, A., Ergon, M., Smartt, S. J., et al. 2015, A&A , 573, A12
Kuncarayakti, H., Maeda, K., Anderson, J. P., et al. 2016, MNRAS, 458, 2063
Lenz, E., & Schlegel, E. M. 2007, AJ, 134, 1821
Milisavljevic, D., Margutti, R., Soderberg, A. M., et al. 2013, ApJ, 767, 71
Montes, M. J., Weiler, K. W., & Panagia, N. 1997, ApJ, 488, 792
Nevalainen, J., David, L., & Guainazzi, M. 2010, A&A, 523, A22
Ng, C.-Y., Zanardo, G., Potter, T. M., et al. 2013, ApJ , 777, 131
Ryder, S. D., Kotak, R., Smith, I. A., et al. 2016, A&A, 595, L9
Ryder, S. D., Staveley-Smith, L., Dopita, M., et al. 1993, ApJ, 416, 167
Schellenberger, G., Reiprich, T. H., Lovisari, L., et al. 2015, A&A, 575, 30
Schlegel, E. M., 1990, MNRAS, 244, 269
Schlegel, D. J., Finkbeiner, D., & Davis, M. 1998, ApJ, 500, 525

Schlegel, E. M., Kong, A., Kaaret, P., DiStefano, R., Murray, S., 2004, ApJ, 603, 644
Schlegel, E. M., Ryder, S., Staveley-Smith, L., et al. 1999, AJ, 118, 2689
Smith, I. A., Ryder, S. D., Böttcher, M., et al. 2007, ApJ, 669, 1130
Smith, M. et al. 2016, XMM-SOC-CAL-TN-0018 [http://xmm2.esac.esa.int/docs/documents/CAL-TN-0018.pdf]
Smith, N. 2014, ARA&A , 52, 487
Snowden, S., Shafer, R., Smith, R., et al. 2016, The XMM-Newton ABC Guide: An Introduction To XMM- Newton Data Analysis, v. 4.6 [http://heasarc.gsfc.nasa.gov/docs/xmm/abc/]
Strüder L. et al., 2001, A&A, 365, L18
Tanaka, M., Nozawa, T., Sakon, I., et al. 2012, ApJ, 749, 173
Turner M. J. L. et al., 2001, A&A, 365, L27
Weng, S.-S., Zhang, S.-N., & Zhao, H.-H. 2014, ApJ, 780, 147
Wilms, J., Allen, A., & McCray, R. 2000, ApJ, 542, 914
Woosley, S. E., Eastman, R. G., Weaver, T. A., & Pinto, P. A. 1994, ApJ, 429, 300